Iron Traffics in Circulation Bound to a Siderocalin (Ngal)-Catechol Complex

Guanhu Bao*, Matthew Clifton*, Trisha M. Hoette, Kiyoshi Mori, Shi-Xian Deng, David Williams, Andong Qiu, Neal Paragas, Thomas Leete, Ritwij Kulkarni, Xiangpo Li, Belinda Lee, Avtandil Kalandadze, Adam J. Ratner, Juan Carlos Pizarro, Kai M. Schmidt-Ott, Donald W. Landry, Kenneth N. Raymond, Roland K.Strong and Jonathan Barasch.

Supplementary Methods

Crystallography, Instruments, HPLC Analysis, Binding Assays, Reduction of Iron by Catechol and Pyrogallol, Generation of Hydroxyradicals, Scn-Ngal:Siderophore:$Iron^{III}$ Traffic, Synthesis of Catechol Sulfonates.

Supplementary Results

Supplementary References

Supplementary Methods

Crystallography X-ray diffraction data sets were collected at the Advanced Light Source 5.0.1 beamline at a wavelength of 1.0 Å and a temperature of 271 K and then processed with HKL2000 software[1] and the Collaborative Computational Project 4 suite of program[2]. Initial difference Fourier phases were calculated directly from the Scn-Ngal:Ent:iron^{III} complex (1L6M) and refined using Refmac[3,4] reflections used to calculate R_{free}[5]. Models were rebuilt using Coot[6]. Ramachandran plots (most favored, additionally allowed, generously allowed, disallowed) were: Catechol:Fe^{III} (3FW4) (84.7, 12.4, 1.2, 1.7), and 4M-Catechol (3FW5) (89.5, 8.9, 0.2, 1.4). The Ramachandran outliers generally occur in the same two residues (Y115 and C175). These same residues are observed outliers in other Siderocalin structures at higher resolution, arguing that these residues are not poorly modeled but truly adopt unfavorable conformations.

Instruments UV was detected with Ultrospec 3300 pro UV/Visible Spectrophotometer (Amersham Biosciences). ESI Mass was detected on a Shimadzu 2010 LCMS spectrophotometer. ^{1}H-NMR spectra were recorded on a Varian-300 MHz instrument in CD_3OD. Radioactivity was measured on a TRI-CARB 2100TR Liquid Scintillation Analyzer from PACKARD. To detect NGAL complexes in serum, we utilized gel filtration (Superdex 200, SMART system) eluted with PBS. Fluorescence quenching measurements were preformed with a Cary Eclipse fluorescence spectrophotometer.

HPLC Analysis Urine was filtered (0.22 μm), extracted 3 times with ethyl acetate and the residue taken up in methanol and analyzed by HPLC and ESI-MS (in negative mode).

In some cases, the sample was hydrolyzed (10% HCl, 90 min, 100 °C). Analytical work (Waters 996) utilized a 2.1 mm × 150 mm, i.d., 3.5 μm beads, C18 SunFire Column with eluant A (0.5% acetic acid in methanol) and eluant B (0.5% acetic acid in water) at a flow rate of 0.5mL/min. Eluant A was increased linearly to 8% within 5min, 15% within 45 min, and then 100% within 5 min, followed by 100% for 10 min. Authentic catechol standardized the results.

To identify the potential sources of catechol, we harvested organs from male 8 week old C57BL/6 mice and dissociating their tissues by dicing and sieving (Fisher Scientific). The cells were then cultured overnight in Minimal Essential Media (1 ml, 37 °C) with L-[5-^{3}H]Tryptophan (5 μCi), L-[4-^{3}H]Phenylalanine (5 μCi), and L-[3,5-^{3}H]Tyrosine (5 μCi). The samples were then hydrolyzed (as above), spiked with non-radioactive catechol (1mg/ml), extracted with EtOAc × 3 and centrifuged to remove tissue fragments. The EtOAc extract was dried (N_2) and the residue dissolved in MeOH/water (1:1) and analyzed on a Waters 600 HPLC, Perkin-Elmer LC-95 UV/Visible spectrophotometer detector and a 4.6 mm × 150 mm, i.d., 3.5 μm beads, C-18 SunFire Column with the same eluants as above. The catechol peak was collected and quantified by HPLC-UV (catechol (x) vs Area Under Curve (y): $y = 5.4206x-0.0141$; $R^2 = 0.998$; limit of detection 0.1 μg/ml).

Binding Assays To test whether urinary compounds bind iron, we spotted the compound (1 nmole, in methanol:water, 50:50) with $^{55}Fe^{III}$ (1 pmole, $Fe^{III}Cl_3$ in water) on Whatman chromatography grade paper (3 mm; #3030917, 8 inches high) and separated bound from free $^{55}Fe^{III}$ by developing the paper chromatogram with water.

To test whether Scn-Ngal formed a complex with iron and the urinary compound, apoScn-Ngal (10 μM), $^{55}Fe^{III}$ (1 μM+cold $Fe^{III}Cl_3$ 9 μM) and the candidate (10 μM) or the positive control. Ent were incubated in 150 mM NaCl, 20 mM Tris (pH 7.4), RT for 60 min. Acidified buffers utilized combinations of Tris HCl and Tris Base. The mixture was then washed 3 or 4 times with the Tris buffer on a YM-10 micron (Millipore) and the retained ^{55}Fe measured with a scintillation counter. Alternatively, the complex was isolated by gel filtration using PD-10 columns in the same buffer (GE Biosciences). For dose-response curves, the candidate was varied from 0-100 μM. Ent:$iron^{III}$ (500 μM) served as a competitor of ^{55}Fe binding.

Reduction of $Iron^{III}$ by Catechol or Pyrogallol The reaction mixture contained 0.24 M potassium phosphate buffer (pH 7.4), 30 mM sodium citrate, 15 μM $Fe^{III}Cl_3$, 50 μM catechols (in 50 mM potassium phosphate buffer, pH 6.5) and 5 mM o-phenanthroline (in ethanol). In some cases Scn-Ngal (60 μg, 15 μM) was added. A time course $iron^{III}$ reduction was monitored by absorbance (512 nm) 5 min after mixing. All spectrophotometric measurements were carried out with a 10 mm light path, with a Ultrospec 3300 pro UV/Visible spectrophotometer at room temperature[2].

Generation of Hydroxyl Radicals Hydroxyl radicals were detected by the conversion of HPF to fluorescein[7]. The reaction mixture contained 0.20 M sodium phosphate buffer (pH 7.4), 30 mM EDTA, 10 μM $Fe^{III}Cl_3$, 30 μM catechols, 2 mM H_2O_2, and 10 μM 3'-(p-hydroxyphenyl) fluorescein (HPF; Invitrogen) or 20 μM F1300 (Invitrogen). In some cases Scn-Ngal (10 μM) was added. After one hour at room temperature, the fluoresence

of the reaction mixture was measured with a LS55 Luminescence Spectrometer, Ex 490 nm, Em 515 nm.

Scn-Ngal:Siderophore:Iron^{III} Traffic To examine the subcellular capture of Scn-Ngal, Alexa568 carboxylic acid succinimidyl ester (Molecular Probes, A20003) coupled Scn-Ngal was prepared according to the manufacturer's instructions with clean up by gel filtration (GE Biotech, PD10) followed by dialysis (Pierce 10K cassette). The protein (50 μg/ml) was added overnight to confluent LLCPK1 cells in serum free DMEM (low glucose) on fibronectin coated filters (BD Sciences, 354492). Cells were fixed in 4% paraformaldehyde/PBS for 3 hrs, 4 °C, stained with TOTO-3 (Molecular Probes, T3604) in PBS with 0.1% TritonX100 for 10 min, mounted in Vectashield and visualized by confocal microscopy (Zeiss LSM510-META inverted confocal laser scanning microscope using a × 40 oil immersion objective and the HeNe laser 543).

To examine whether Scn-Ngal:catechol:Fe modifies iron responsive genes, LLCPK1 (3×10^5 cells per well) were transfected with 5'IRE-DsEYFP (2 hrs half life)[8] and cultured with desferoxamine (DFO, 25 μM) and holo-transferrin (50 μg/ml) with ferric ammonium citrate (50 μM) as negative and positive controls, respectively, or with Scn-Ngal:catechol-Fe (100 or 500 μg/ml) in DMEM (low glucose). After 16 hrs, the cells were either fixed (4% paraformaldehyde/PBS for 3 hrs, 4 °C) and then examined by fluorescence microscopy (× 40 oil immersion objective) or by first lysing the cells using freeze-thaw cycles in ice-cold PBS with a cocktail of protease inhibitors (Roche, 11836145001) and then quantifying fluorescence (Ex 513nm and Em 527nm), normalized for protein concentration using a BCA method (Pierce, 23227)

Synthesis of Catechol Cyclic Sulfate and Catechol Monosulfate Sodium. We used the same method described in the literature. To synthesize catechol cyclic sufonate[9], catechol (1.1 g) in pyridine/hexane (1.6 g/10ml) was treated with sulfuryl chloride/hexane (1.36 grams/2ml) at -5 °C overnight, after which the reaction was warmed for 6 hrs. The upper layer was decanted, and the lower layer washed twice with EtOAc. The combined washes and the upper layer were then washed with 5% $Cu(OAC)_2H_2O$, and the absence of catechol demonstrated by TLC (hexane- EtOAc, 3:l) (Rf = 0.14). The solution was then dried over magnesium sulfate and concentrated, yielding 1.8 g of amber liquid. Recrystallization from hexane yielded 0.8 g of catechol cyclic sulfate, long colorless needles, mp 35-37 °C (lit.s mp 34-35 °C). ^{1}H NMR (300 MHz, CD_3OD, δ ppm): 7.31 (2H, *m*), 7.24(2H, *m*), (catechol: 6.24 and 6.41 ppm). To synthesize catechol monosulfate sodium[10], catechol cyclic sulfate (100mg) was hydrolyzed in acetonitrile/0.1 N NaOH (1.2 ml/1 ml) for 3 hrs, and then extracted with chloroform and dried with ethanol. Catechol monosulfate sodium was obtained as white powder (70mg, 56.8%). ^{1}H NMR (300 MHz, CD_3OD, δ ppm): 7.27 (dd, J = 8.1, 1.8 Hz, 1H), 7.04 (td, J = 7.8, 1.5 Hz, 1H), 6.79 (dd, J = 8.1, 1.5 Hz, 1H), 6.62 (td, J = 7.8, 1.5 Hz, 1H). Analytical data matched previously published values.

Supplementary results

Supplementary Figure 1 Urine contains small molecules that bind iron. Low molecular weight urine (< 3 KDa) samples (1X = 5 µl; 3X = 15 µl) and $^{55}Fe^{III}$ (1 pm) were spotted and dried together on a paper chromatogram. The chromatogram was then developed in water. The direction of the solvent flow is indicated by the arrow. $^{55}Fe^{III}$ was mobilized by the urine sample in a dose dependent fashion. AKI-acute kidney injury; CKD-chronic kidney disease. (n = 3, independent experiments).

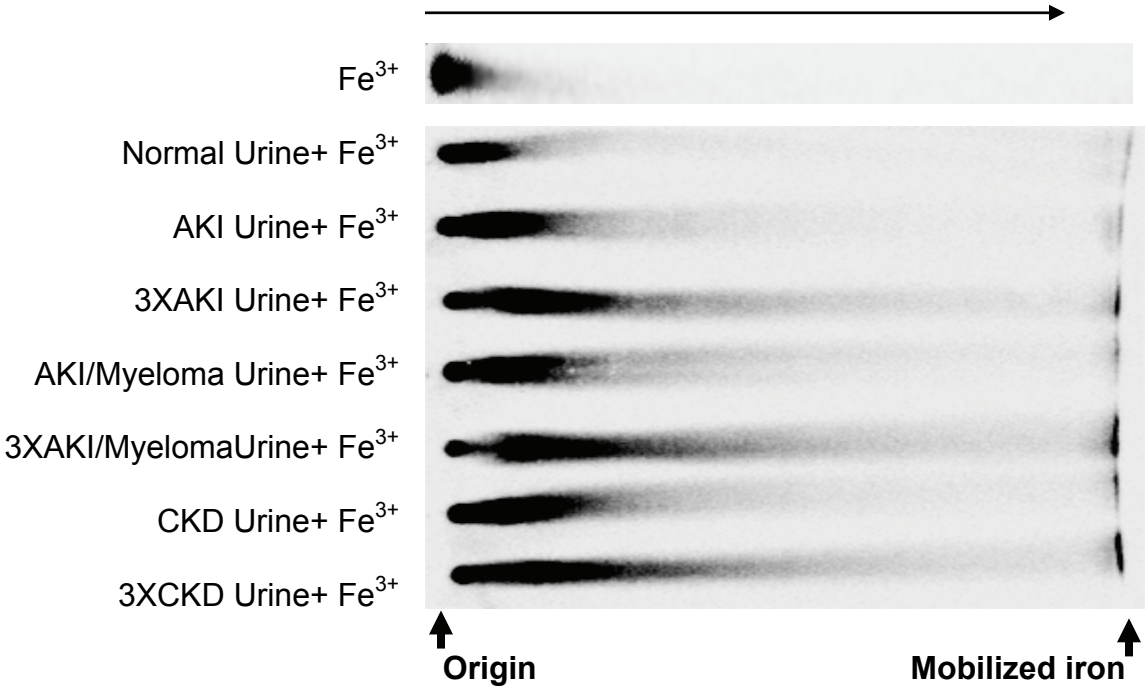

Supplementary Figure 2 Urinart compounds enhance the association of iron^{III} and Scn-Ngal. $^{55}Fe^{III}$ (1 μM + 9 μM cold $Fe^{III}Cl_3$) was combined with apo Scn-Ngal (10 μM), or with apo Scn-Ngal (10 μM) mixed with either Ent (10 μM) or low molecular weight human or mouse urine (100 μg; < 3 KDa) or its extracts (100 μg) at pH 7.0. The mixtures were then washed 3 times on a 10K microcon. $^{55}Fe^{III}$ retention depended on the bacterial (Ent) or urinary (unknown) cofactors. Ent (P = 0.021; two tailed t-test), human urine (P = 0.034; two tailed t-test), mouse urine (P = 0.0008; two tailed t-test) or an ethylacetate extract of human urine (P = 0.0007; two tailed t-test) significantly increased iron retention by apo-Scn-Ngal. Each assay was repeated 3 times with different preparations of Scn-Ngal. (Mean±s.d.; * P < 0.05; ** P < 0.005; ns, non-significant differences compared with apo Scn-Ngal).

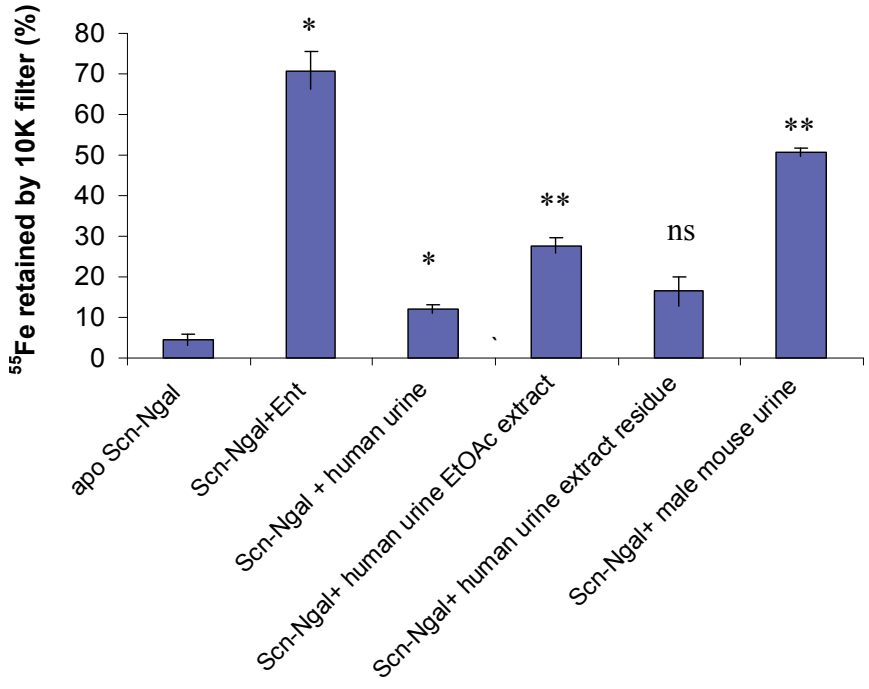

Supplementary Figure 3 Stable Association of Catechol:$^{55}Fe^{III}$ with Scn-Ngal. Apo Scn-Ngal (10 μM), catechol (10 μM), and iron (1 μM $^{55}Fe^{III}$ + 9 μM cold $Fe^{III}Cl_3$) were washed repetitively on a 10K microcon filter. After each wash, 5% of the sample was measured by scintillation counting and the values corrected for serial sampling. The catechol complex retained iron to the same extent as did Ent and 2,3-dihydroxybenzoic acid (not shown), which are proven ligands of Scn-Ngal. A representative experiment is shown.

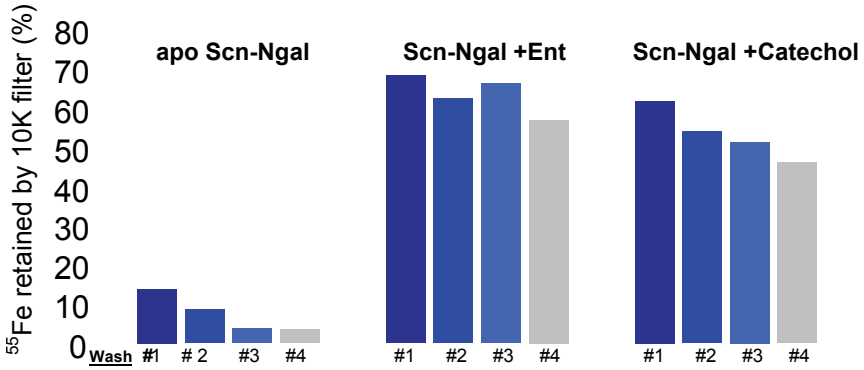

Supplementary Figure 4 Stable Association of Catechol:$^{55}Fe^{III}$ with Scn-Ngal. Apo Scn-Ngal (10 μM), catechol (10 μM), and iron (1 μM $^{55}Fe^{III}$ + 9 μM cold $Fe^{III}Cl_3$) were mixed and then rapidly gel-filtered on PD-10 columns. The Scn-Ngal:catechol:$^{55}Fe^{III}$ complex was recovered. Apo-Scn-Ngal served as a negative control and apo-Scn-Ngal:Enterochelin served as a positive control. Note that free enterochelin:$^{55}Fe^{III}$ eluted early due to its high molecular weight (719 Da), whereas free catechol:$^{55}Fe^{III}$ (110 Da) was entirely excluded. A representative experiment is shown.

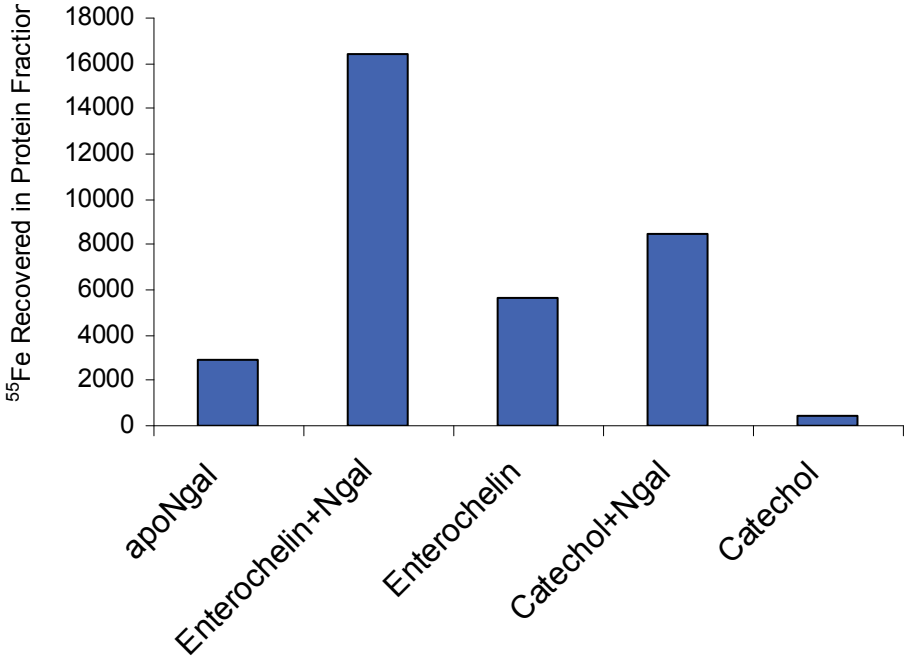

Supplementary Figure 5 Screening of compounds found in human urine that potentially chelate iron. (**a**) $^{55}Fe^{III}Cl_3$ was spotted on a paper chromatogram together with the candidate siderophore. Interaction between $^{55}Fe^{III}$ and the candidate siderophore was detected by the mobilization of iron^{III} to the front of the paper chromatogram (direction of the arrow). "Fe only" served as a negative control; "Ent" served as a positive control (n = 3 independent assays). Note that only a few compounds mobilized Fe^{III}. (**b**) Iron retention by complexes of Scn-Ngal and candidate siderophoreswas detected by adding $^{55}Fe^{III}$, (n = 4-7 independent preparations of Scn-Ngal). 2,3 DHBA served as a positive control. Note the saturation of Scn-Ngal by the small catechols. (**c**) Iron^{III} retention by complexes of Scn-Ngal and candidate siderophores was detected by adding $^{55}Fe^{III}$ with (light blue bars, n = 4-5) or without (dark blue bars, n = 4-5 independent assays) the addition of a 50 fold molar excess of Ent that was presaturated with non-radioactive iron. (**d**) Wild type Scn-Ngal (dark blue bars, n =3-4 independent assays) was also compared with Scn-Ngal K125A, K134A mutant (grey bars, n =3-4 independent assays). Apo-Scn-Ngal served as the negative control and Ent and 2,3 DHBA served as positive controls. Each experiment used an independent preparation of Scn-Ngal. (**c and d**) Data represent mean ± s.d., and statistical significance (*$P < 0.05$; **$P < 0.005$; ***$P < 10^{-4}$; ****$P < 10^{-5}$) was assessed by two tailed Students *t*-test, and ns signifies non-significant differences in the comparisons between wild type *vs* mutant Scn-Ngal and between presence *vs* absence of the Ent:cold-Fe^{III} competitor.

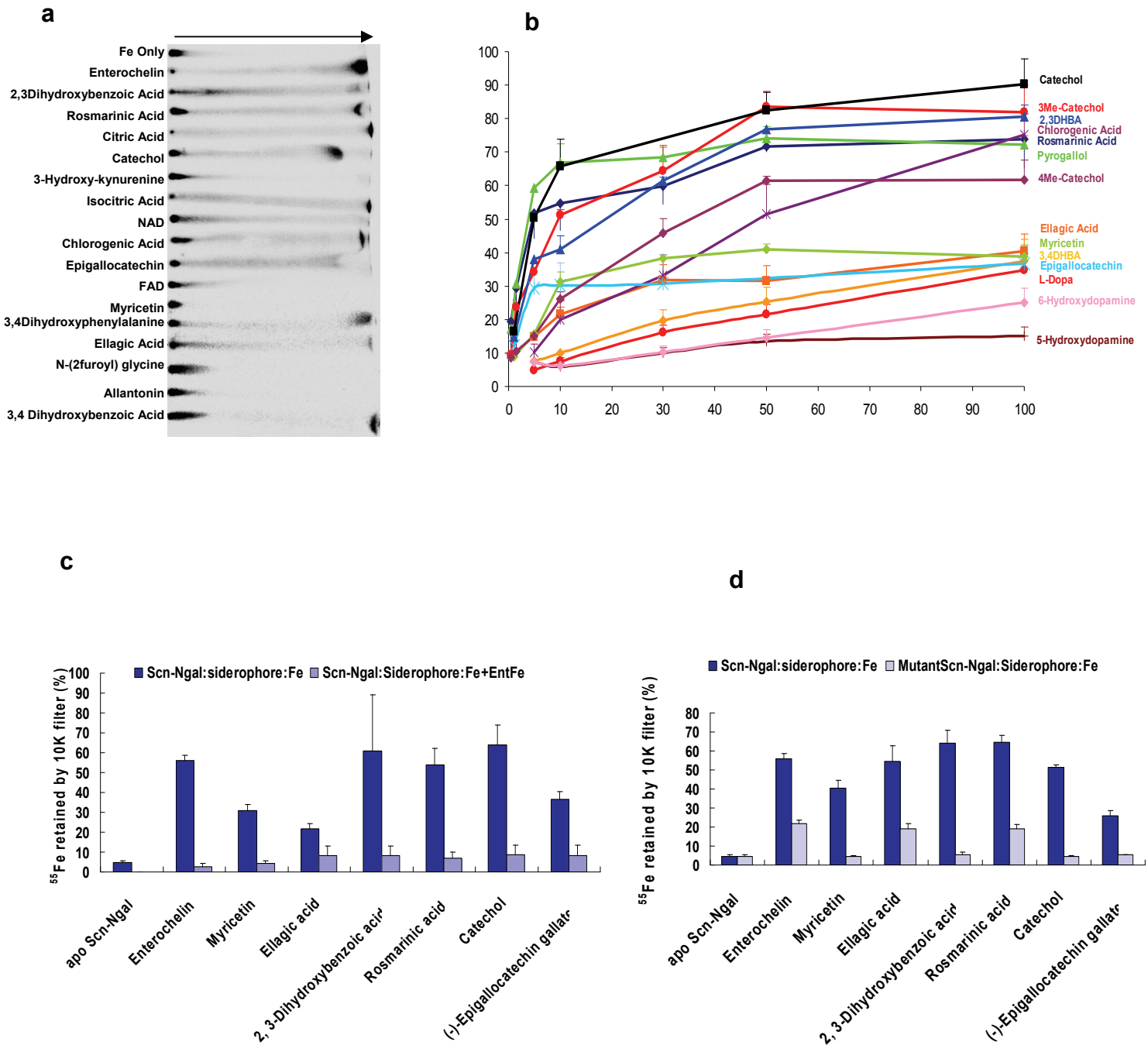
a
Fe Only
Enterochelin
2,3Dihydroxybenzoic Acid
Rosmarinic Acid
Citric Acid
Catechol
3-Hydroxy-kynurenine
Isocitric Acid
NAD
Chlorogenic Acid
Epigallocatechin
FAD
Myricetin
3,4Dihydroxyphenylalanine
Ellagic Acid
N-(2furoyl) glycine
Allantonin
3,4 Dihydroxybenzoic Acid
b
Catechol
3Me-Catechol
2,3DHBA
Chlorogenic Acid
Rosmarinic Acid
Pyrogallol
4Me-Catechol
Ellagic Acid
Myricetin
3,4DHBA
Epigallocatechin
L-Dopa
6-Hydroxydopamine
5-Hydroxydopamine
c
Scn-Ngal:siderophore:Fe
Scn-Ngal:Siderophore:Fe+EntFe
55Fe retained by 10K filter (%)
apo Scn-Ngal
Enterochelin
Myricetin
Ellagic acid
2, 3-Dihydroxybenzoic acid
Rosmarinic acid
Catechol
(-)-Epigallocatechin gallate
d
Scn-Ngal:siderophore:Fe
MutantScn-Ngal:Siderophore:Fe
55Fe retained by 10K filter (%)
apo Scn-Ngal
Enterochelin
Myricetin
Ellagic acid
2, 3-Dihydroxybenzoic acid
Rosmarinic acid
Catechol
(-)-Epigallocatechin gallate

Supplementary Figure 6 Binding spectrum of catechol:Fe^{III} and Scn-Ngal. At pH 7.0 (upper graph) catechol:Fe^{III} generates a spectrum (λ_{max} = 575 nm, dark blue line) consistent with the formation of di-catechol:iron ($Fe^{III}L_2$) complexes. The addition of Scn-Ngal however resulted in a shift of the spectrum (λ_{max} = 498 nm, red curve) consistent with formation of a tris-catecholate complex ($Fe^{III}L_3$). In contrast, little, if any $Fe^{II}L_2$ or $Fe^{II}L_3$ formed in solution (light blue) or within the Scn-Ngal calyx (pink), and these small deflections were abolished by the addition of ascorbate (tan and acqua, respectively). No spectral changes were found at pH 4.0 (lower graph), consistent with the pH sensitivity of the complexes.

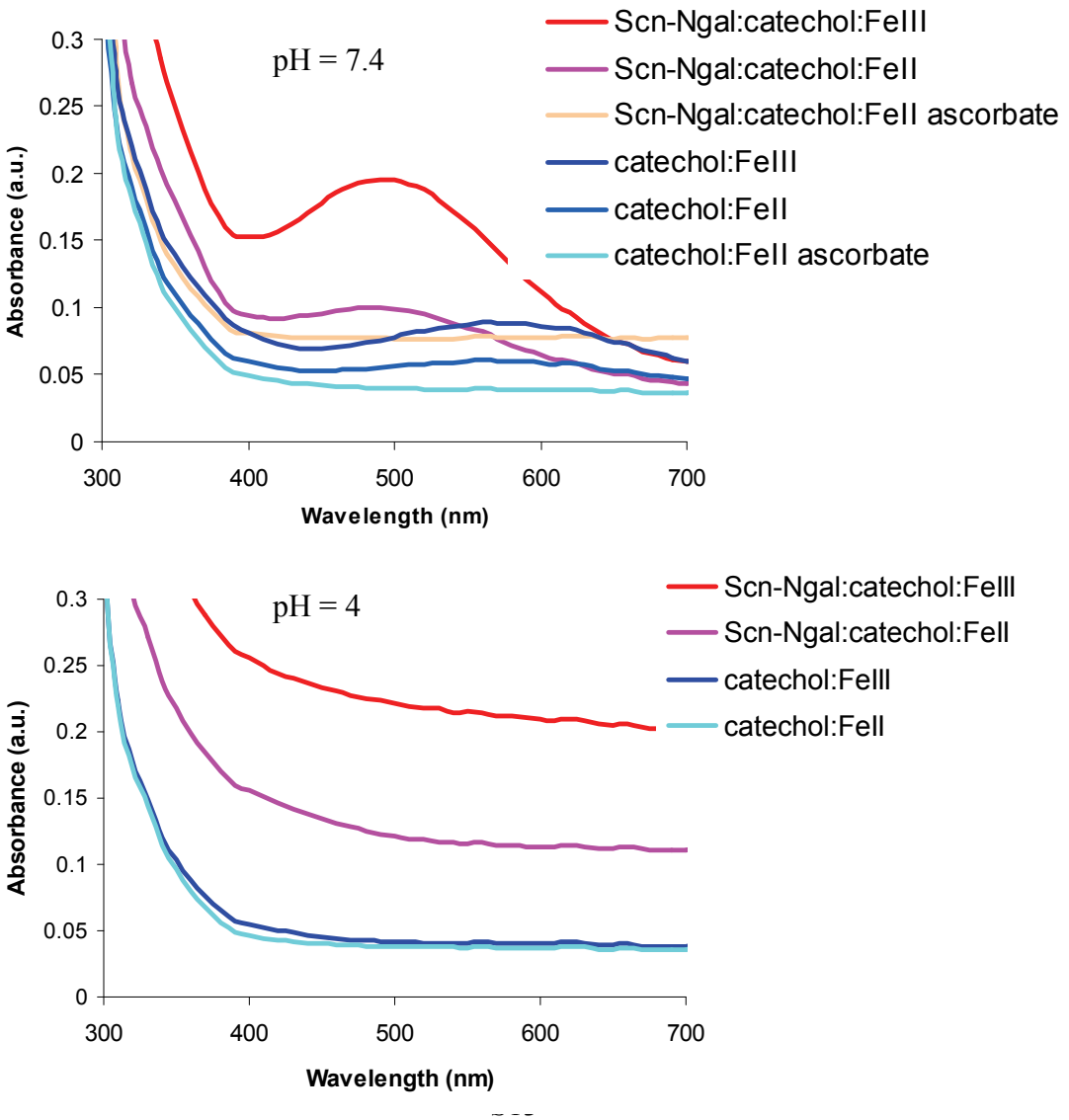

Supplementary Figure 7 Relative position of catechol and 4-methylcatechol in molecule A (left) and molecule C (right). In molecule A, there is a rotation of 120°, and 4-methylcatechol shifts up approximately 1.4 Å towards the outside of the calyx. In molecule C, the rings rotate 80° and 4-methylcatechol shifts up approximately 1 Å towards the outside of the calyx. In both molecules A and C, when 4-methylcatechol (iron = orange) serves as the ligand iron (orange) is shifted towards the center of the calyx compared to its position when catechol serves as the ligand (yellow).

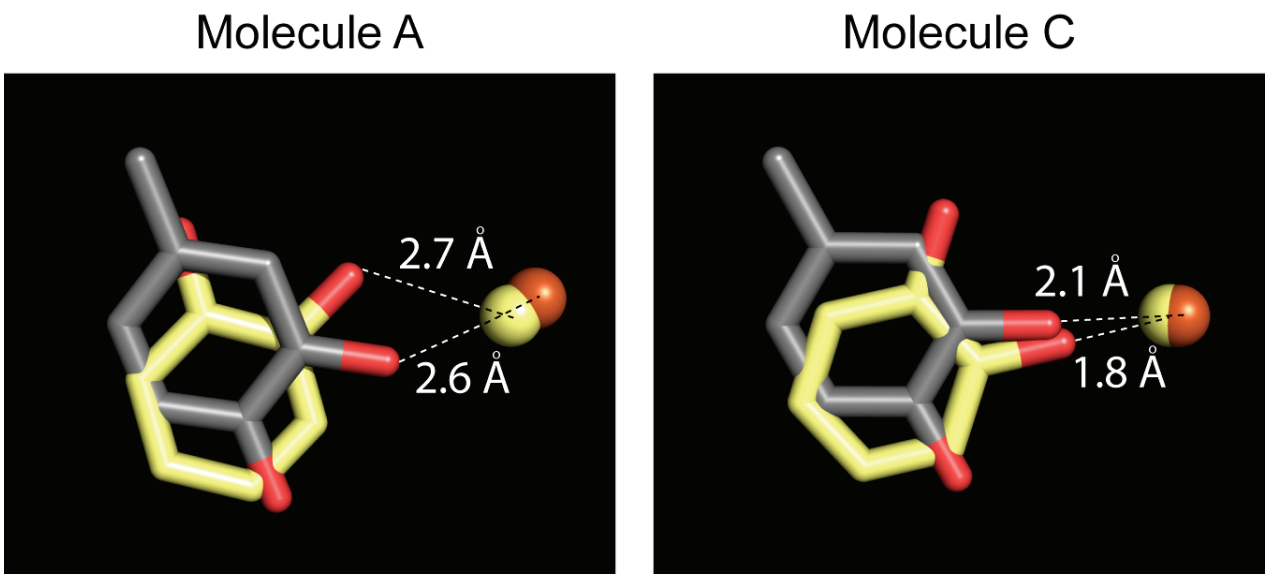

Supplementary Figure 8 Superimposition of Catechol and Bacterial Siderophores Ent and Carboxymycobactin from Scn-Ngal structures. Catechol (left) and 4-methylcatechol (right). Catechol:iron^{III} is shown in light yellow (molecule A) and dark yellow (molecule C), catechol rings from Ent are shown in light green (molecule A) and dark green (molecule C), 4-methylcatechol:iron^{III} is shown in light gray (molecule A) and dark gray (molecule C), phenol oxazoline groups from Cmb (1X89) are shown in light blue (molecule A) and dark blue (molecule C). For clarity only the iron binding portion of the ligands are shown from each structure.

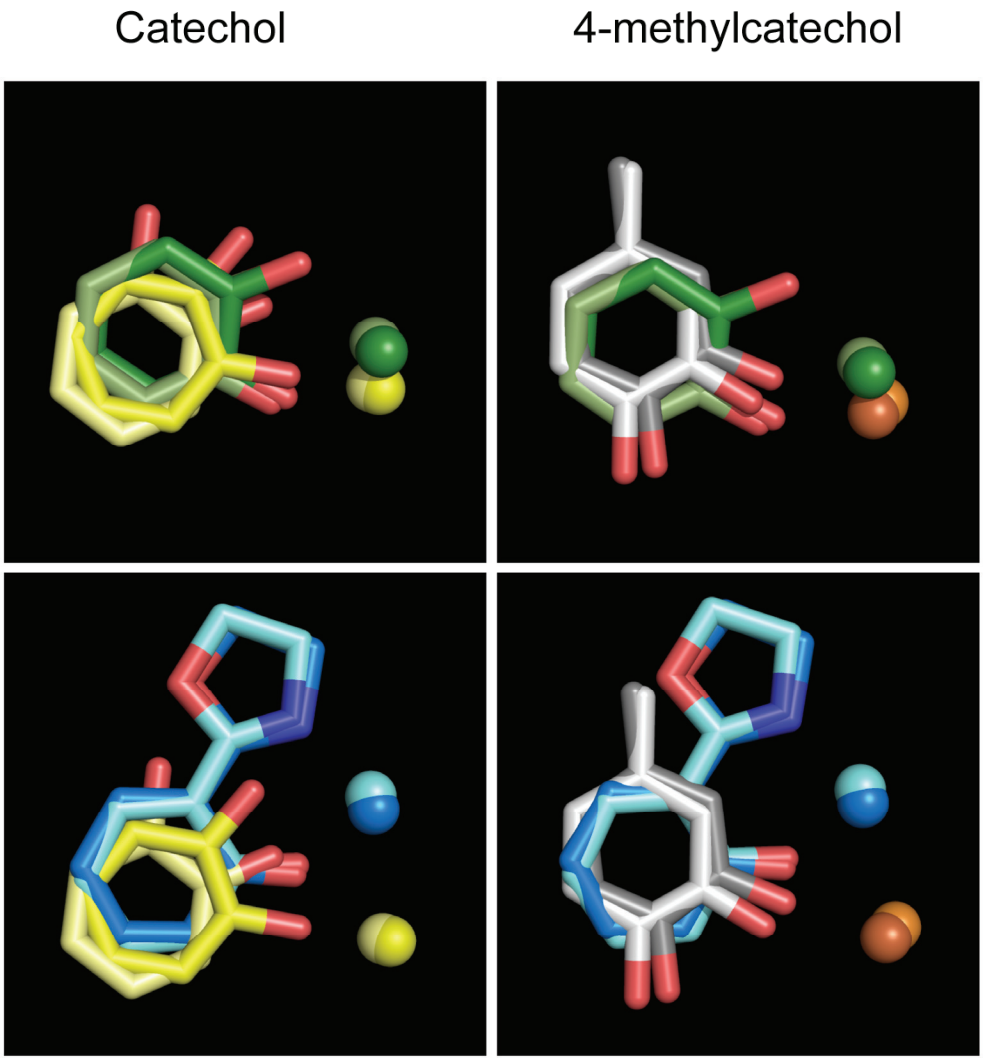

Supplementary Figure 9 The presence of chloride in the Scn-Ngal calyx. The electrostatic surface representation of Scn-Ngal bound to catechol:Fe^{III} is represented by positive (blue), neutral (white), and negative (red) charges in the calyx. Chloride atoms (green) are likely to compensate for the positive charge of Fe^{III} (orange).

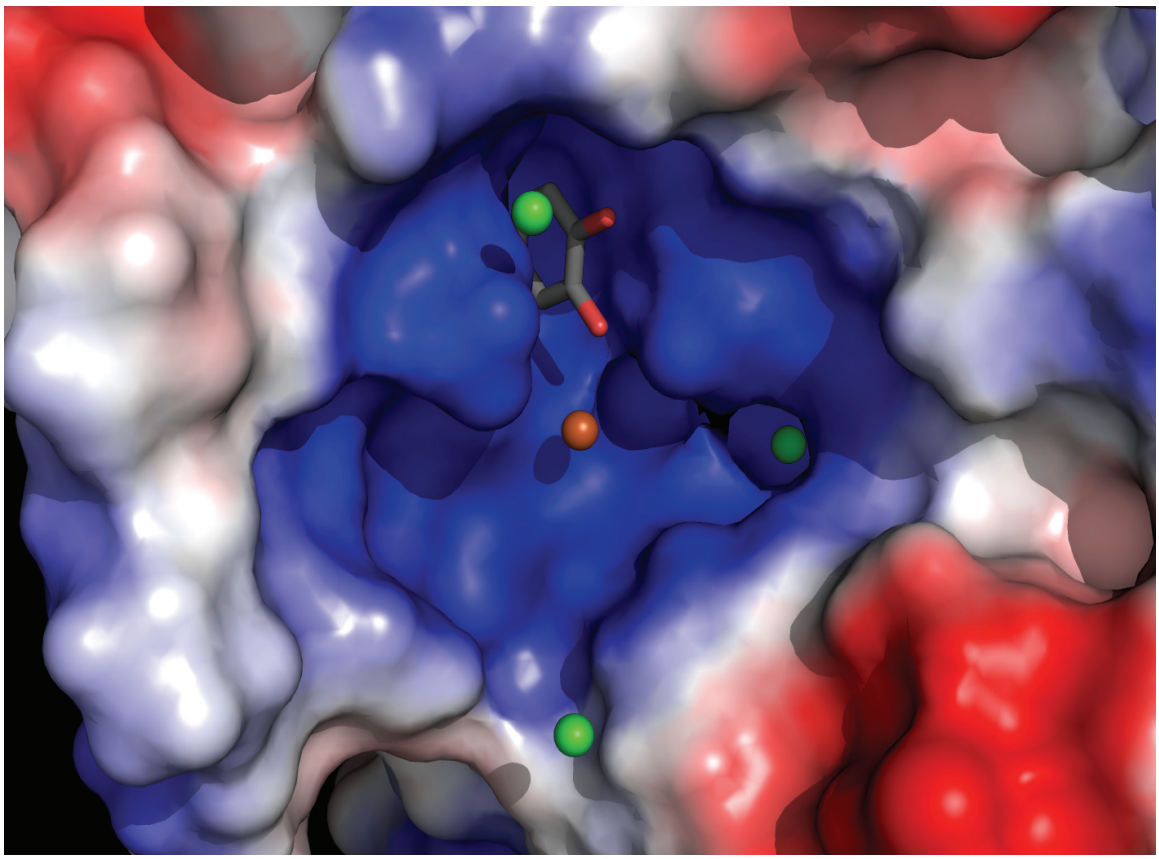

Supplementary Figure 10 Urine was collected from both wild type and megalin deleted mice[11]. Scn-Ngal was detected by immunoblot using polyclonal anti-mouse Scn-Ngal antibodies[12].

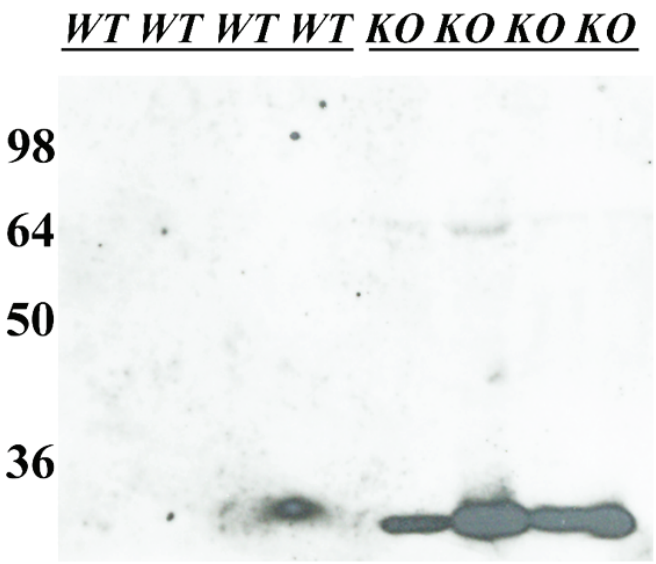

Supplementary Fig. 11 Scn-Ngal effectively chelates $iron^{III}$. (**a**). Catechol and pyrogallol (black and dark green, respectively) reduced Fe^{III} to Fe^{II}, which we detected using phenanthroline absorbance (512 nm). The addition of stoichiometric quantities of Scn-Ngal significantly decreased phenanthroline absorbance of both catechol complexes (grey and light green, respectively; catechol+$FeCl_3$±Scn-Ngal: $P<10^{-4}$; pyrogallol+$FeCl_3$±Scn-Ngal: $P< 0.005$, two-tailed *t*-test, n=4) (**b**) Conversion of HPF to fluorescein (Ex 490 nm, Em 515 nm) was detected in the presence of catechol, $iron^{III}$ and H_2O_2 (dark blue line), but the addition of Scn-Ngal blocked the reaction (light blue line; HPF+ catechol+$FeCl_3$ ± Scn-Ngal: $P<10^{-5}$, n=3). Catechol sulfonate was inactive (blue line). Fluorescein (F) was not affected by the addition of Scn-Ngal (green lines). Data represent mean ± s.d., n=3 independent experiments

a

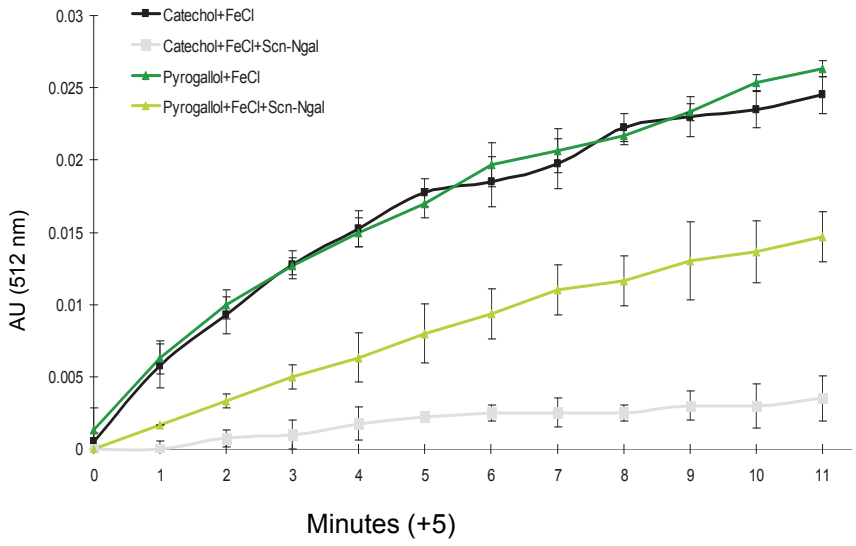
Catechol+FeCl
Catechol+FeCl+Scn-Ngal
Pyrogallol+FeCl
Pyrogallol+FeCl+Scn-Ngal
AU (512 nm)
0.03
0.025
0.02
0.015
0.01
0.005
0
0 1 2 3 4 5 6 7 8 9 10 11
Minutes (+5)

b

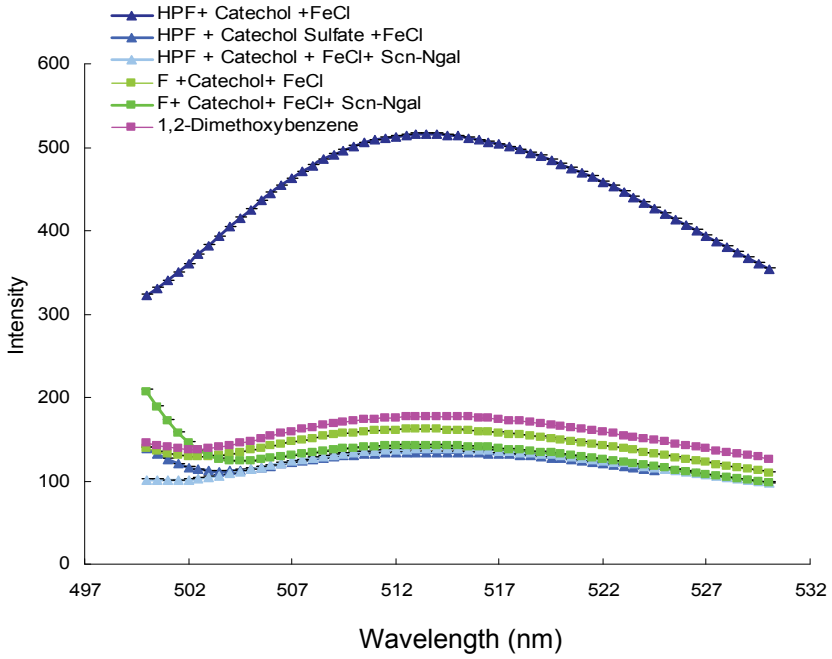
HPF+ Catechol +FeCl
HPF + Catechol Sulfate +FeCl
HPF + Catechol + FeCl+ Scn-Ngal
F +Catechol+ FeCl
F+ Catechol+ FeCl+ Scn-Ngal
1,2-Dimethoxybenzene
Intensity
600
500
400
300
200
100
0
497 502 507 512 517 522 527 532
Wavelength (nm)

Supplementary Figure 12 Scn-Ngal:catechol:Fe upregulates iron dependent gene expression in LLCPK cells. (**a**) Cells were grown on fibronectin coated filters to confluence and then incubated with Alexa-568 coupled Scn-Ngal (50μg/mL, red) overnight in serum free MEM. After fixation, nuclei were stained with Toto-3 (blue). (**b-g**) LLCPK cells were transfected with an iron-responsive reporter called 5'IRE-YFP which detects iron by enhanced translation of YFP. (**b**) Cells were then incubated with deferoxamine iron chelator DFO (25 μM), holo-transferrin (50 μg/ml) with ferric ammonium citrate (50 μM), Scn-Ngal:catechol-Fe (100 or 500 μg/ml) in DMEM (low glucose) for 16 hrs. YFP was then detected by spectrophotometry (Ex 513 nm, Em 527 nm) normalized to cell protein in lysed cells. Data represent mean±s.d., n = 3 independent assays; $^{**}P < 0.005$, two tailed *t*-test Scn-Ngal *vs* DMEM. (**c-g**) YFP was also detected by fluorescence microscopy (40x oil immersion lens) in 3 independent assays. Images are representative of all of the fields in the 2.5 cm diameter well.

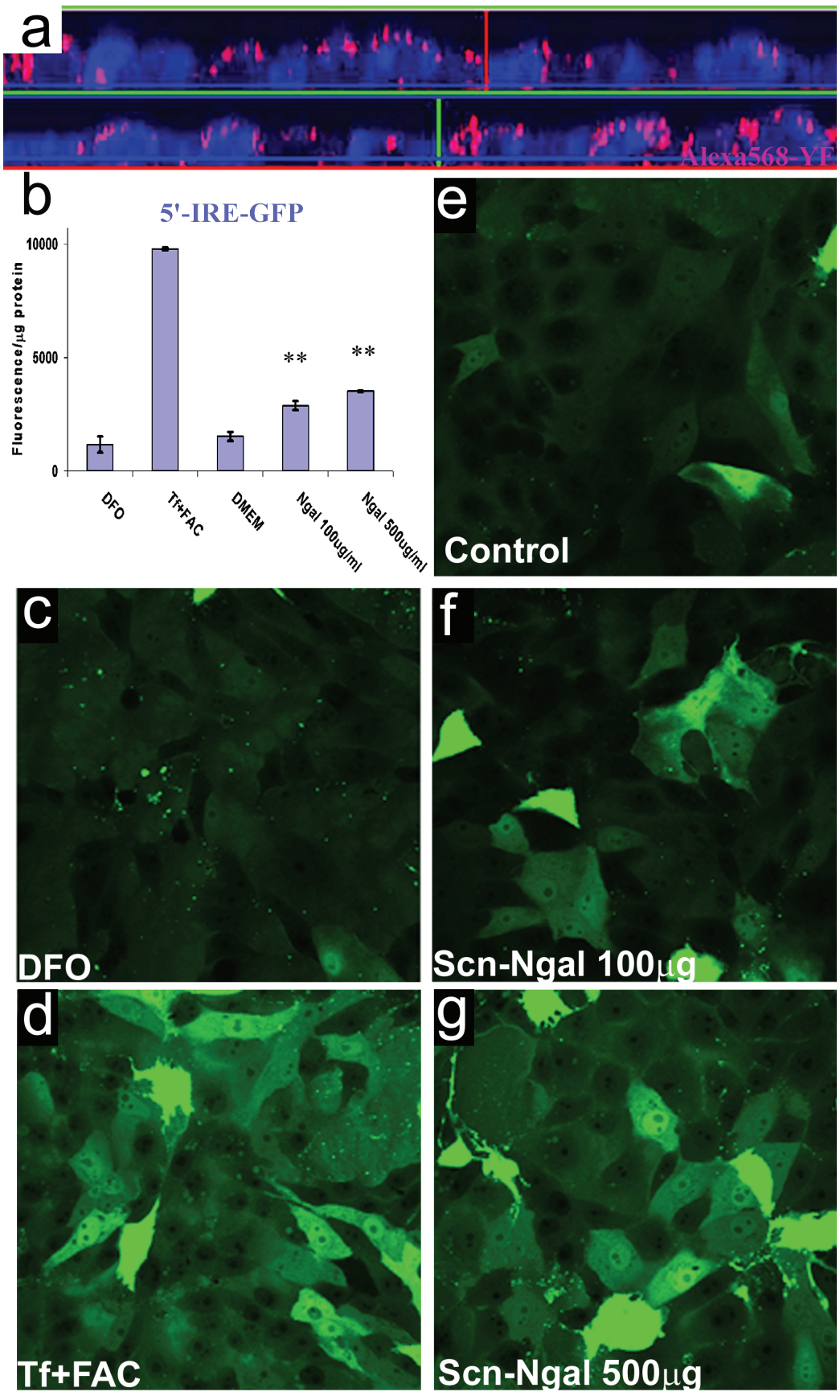
a
Alexa568-YF
b
5'-IRE-GFP
Fluorescence/μg protein
10000
5000
0
**
**
DFO
Tf+FAC
DMEM
Ngal 100ug/ml
Ngal 500ug/ml
e
Control
c
DFO
f
Scn-Ngal 100μg
d
Tf+FAC
g
Scn-Ngal 500μg

Supplementary Figure 13 Conversion of tyrosine to catechol (*). Dissociated intestinal cells (37 °C, overnight) converted ^{3}H-tyrosine into a compound migrating with unlabeled catechol (black line, *fraction 25-27, C-18 HPLC analysis) as well as a second metabolite (fraction 9-11); *0*-methylation of the extract (bright blue) abolished these peaks. The authenticity of the peak was further established by its mobility on TLC, before and after dimethylation compared with authentic catechol (data not shown).

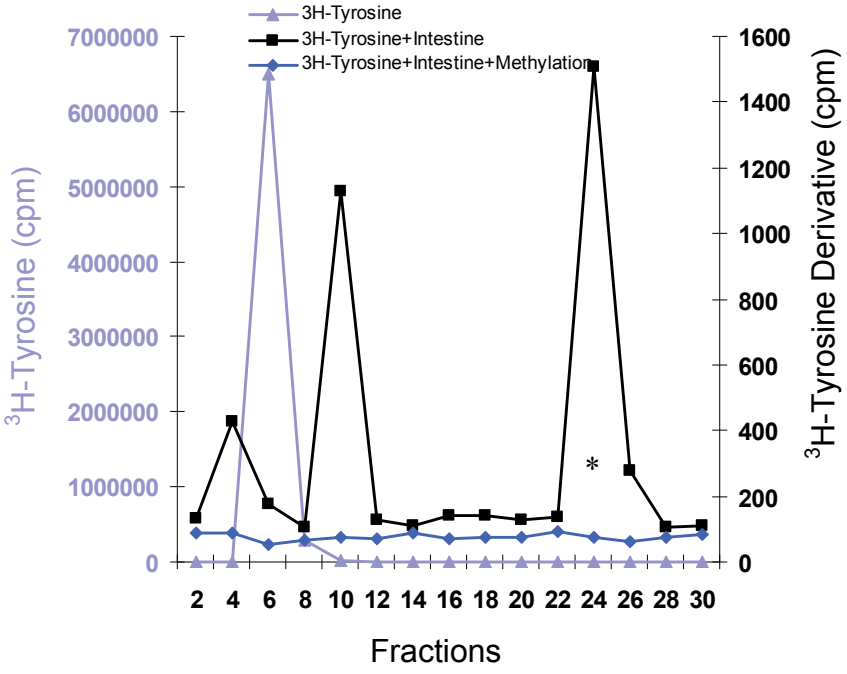

Supplementary Figure 14 Identification of catechol in human urine. Urine contains small molecules that bind iron^{III} and Scn-Ngal. The most active fraction (urine EtOAc extract) contained catechol (retention time: 25.5-26 min) as demonstrated by the addition of authentic catechol standards. HPLC-UV 216 nm, 274 nm; C-18 column eluted with a gradient of methanol in 0.5% acetic acid.

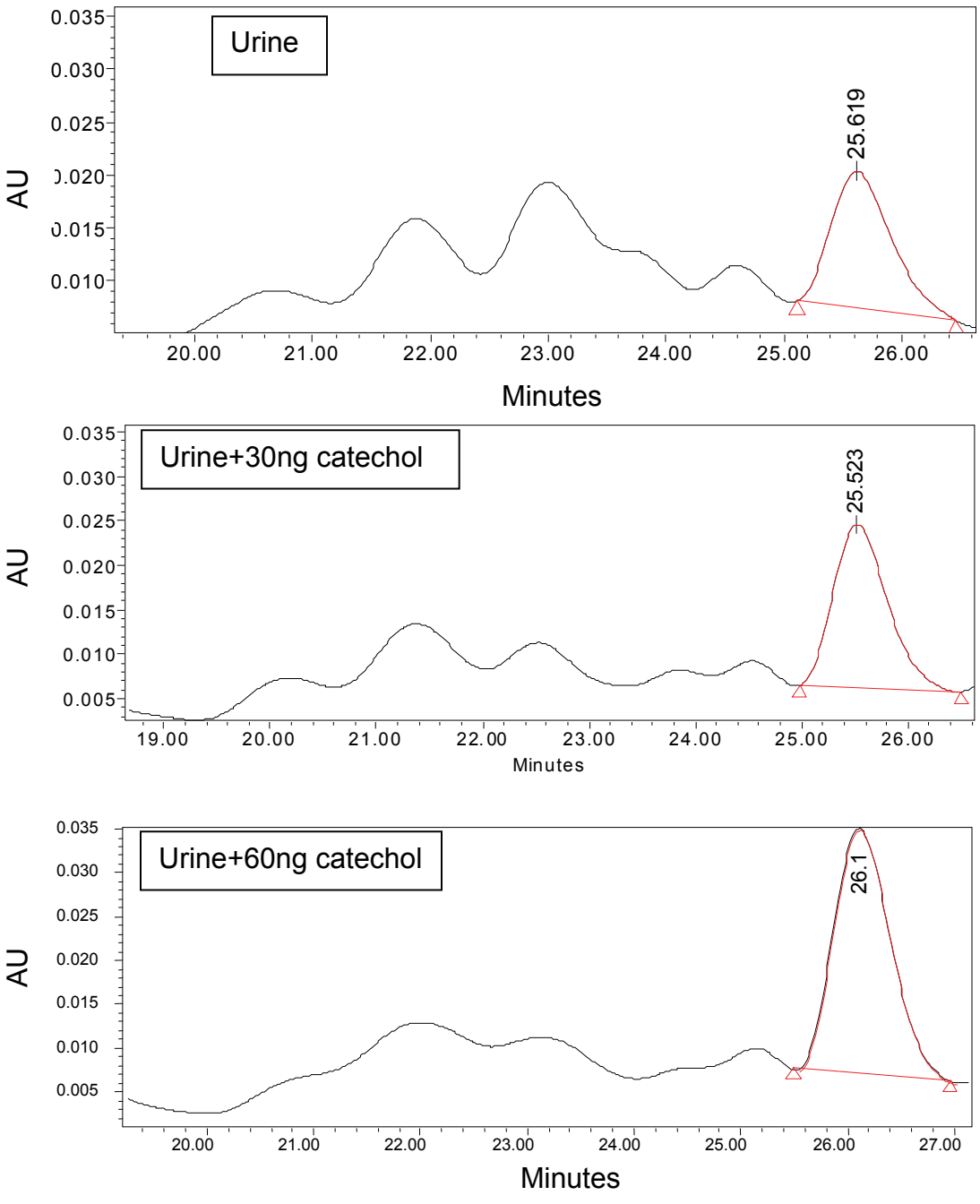

Supplementary Figure 15 Identification of catechol in an ethylacetate extract of human urine by ESI Mass Spectroscopy. Note the catechol mass $[M-H]^-$, presumptive dimer $[2M-H]^-$ and solvent complexes.

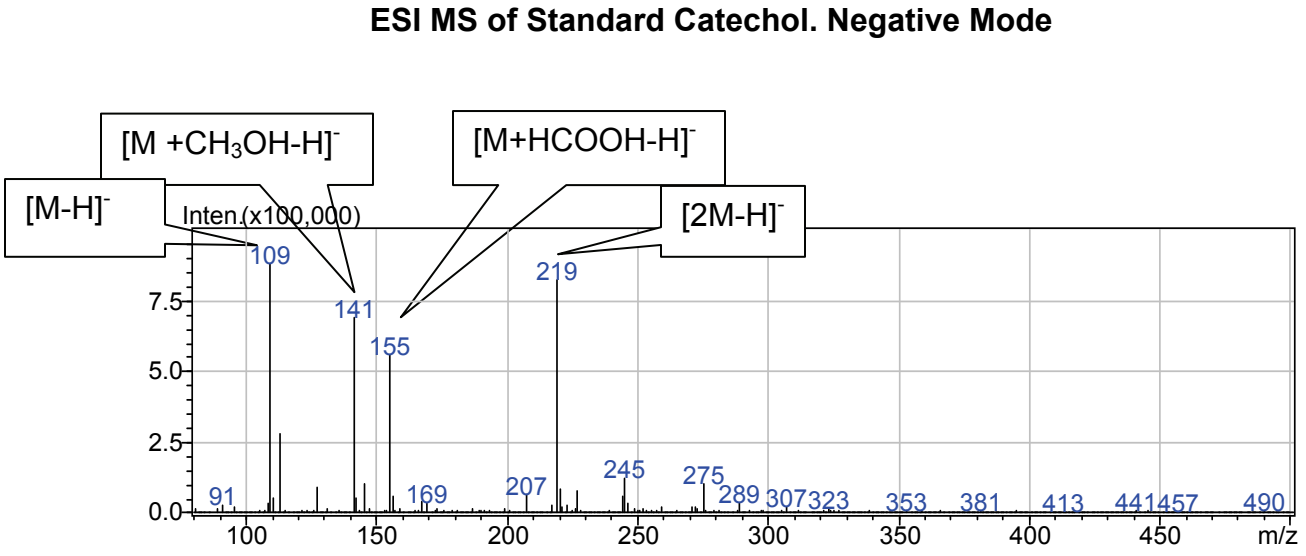

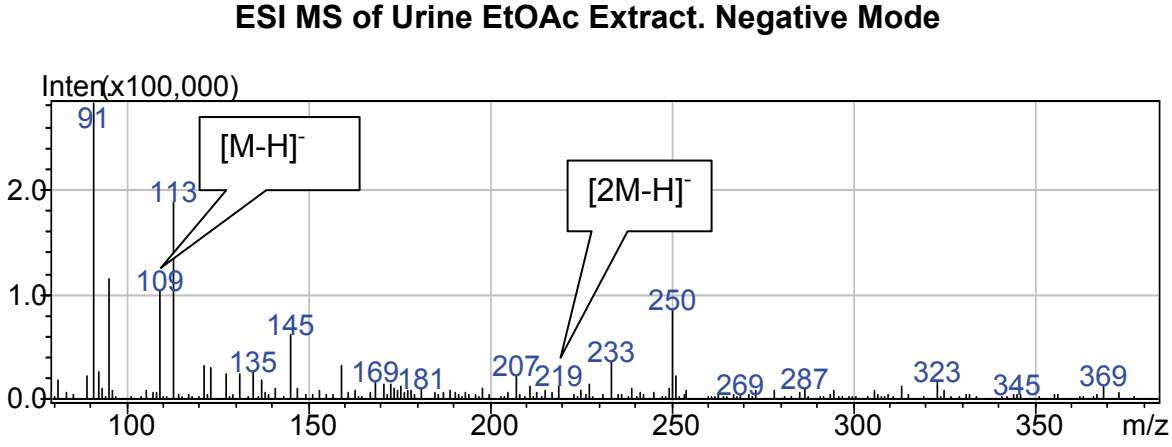

Supplementary Table 1: Binding Energies

Theoretical quadrupole moments (Θ_{ZZ}, optimization and calculation at the RHF/6-311G** level of theory) and cation binding energies (p-Na^+, calculated at the MP2/6-311++G** and corrected for BSSE) for aromatic units studied.

	Θzz	π–Na^+ BE (kcal/mol)
Catechol	-9.64	-30.89
3-methyl catechol	-10.22	-21.21
4-methyl catechol	-9.69	-21.04
Pyrogallol	-9.95	-19.64
2,3-DHBA	-6.46	-16.18
3,4-DHBA	-8.44	-15.92
Quinone	0.59	-1.05

Supplementary Table 2: Crystallographic Statistics

	Fe-catechol	Fe-4-methyl-catechol	Fe-3-methyl-catechol	Fe-pyrogallol	Fe-caffeic acid	Fe-rosmarinic acid
Data collection						
Space group	$P4_12_12$	$P4_12_12$	$P4_12_12$	$P4_12_12$	$P4_12_12$	$P4_12_12$
Cell dimensions						
a, *b*, *c* (Å)	115.4, 115.4, 118.8	114.9, 114.9, 119.6	115.1, 115.1, 118.6	116.3, 116.3, 120.8	114.4, 114.4, 119.2	114.8, 114.8, 118.7
α, β, γ (°)	90, 90, 90	90, 90, 90	90, 90, 90	90, 90, 90	90, 90, 90	90, 90, 90
Resolution (Å)	50-2.3 (2.38-2.3)	50-2.3 (2.38-2.3)	50-3.25 (3.37-3.25)	50-2.7 (2.8-2.7)	50-2.43 (2.52-2.43)	35-2.4 (2.53-2.44)
R_{merge}	0.055 (0.39)	0.048 (0.40)	0.135 (0.39)	0.063 (0.35)	0.051 (0.28)	0.057 (0.27)
$I / \sigma I$	31.5 (5.09)	25.0 (5.39)	7.28 (2.96)	23.9 (6.69)	15.2 (7.5)	21.4 (5)
Completeness (%)	99.9 (100)	99.9 (100)	98.1 (100)	95.5 (99.5)	99.5 (95)	99.9 (98.9)
Redundancy	7.9 (6.8)	8.0 (7.8)	3.5 (3.4)	5.3 (5.1)	14.1 (11.4)	14.4 (14.2)
Refinement						
Resolution (Å)	2.3	2.3	-	-	-	-
No. reflections	36375 (3562)	35984 (3519)	-	-	-	-
R_{work} / R_{free}	25.6 / 28.3	24.4 / 29.0	-	-	-	-
No. atoms	4057	4339	-	-	-	-
Protein	3704	3973	-	-	-	-
Ligand/ion	99	92	-	-	-	-
Water	243	270	-	-	-	-
B-factors			-	-	-	-
Protein (A, B, C)	41.5, 88.5, 32.9	38.3, 69.0, 32.7	-	-	-	-
Ligand/ion	67.9	61.1	-	-	-	-
Water	47.8	47.5	-	-	-	-
R.m.s. deviations			-	-	-	-
Bond lengths (Å)	0.005	0.005	-	-	-	-
Bond angles (°)	0.925	0.941	-	-	-	-

* Statistics for each data set is based on a single crystal
* Highest-resolution shell is shown in parentheses.

Supplementary References

1. Otwinowski, Z. & Minor, W. *Processing of X-ray Diffraction Data Collected in Oscillation Mode*, Methods in Enzymology, Volume 276: Macromolecular Crystallography, part A, C.W. Carter, Jr. & R. M. Sweet, Eds. (Academic Press, New York,1997), pp.307-326.

2. Collaborative Computational Project, Number 4. "The CCP4 Suite: Programs for Protein Crystallography." *Acta Cryst*. **D50**, 760-763 (1994).

3. Murshudov, G.N., Vagin, A.A. & Dodson, E.J. Refinement of macromolecular structures by the maximum-likelihood method. *Acta Cryst*. **D53**, 240-255 (1997).

4. Laskowski, R.A., MacArthur, M.W., Moss, D.S. & Thornton, J.M. PROCHECK: a program to check the stereochemical quality of protein structures. *J. Appl. Cryst*. **26**, 283-291 (1993).

5. Kleywegt, G.J. & Brugner, A.T. Checking your imagination: applications of the free R value, *Structure* **15**, 897-904 (1996).

6. Emsley, P. & Cowtan, K. Coot: Model-building tools for molecular graphics, *Acta Cryst.* **D60**, 2126-2132 (2004).

7. Setsukinai, K. *et al*. Development of novel fluorescence probes that can reliably detect reactive oxygen species and distinguish specific species. *J. Biol. Chem*. **278**, 170-3175 (2003).

8. Li, J.Y. *et al*. Detection of intracellular iron by its regulatory effect. *Am. J. Physiol. Cell Physiol*. **287**, C1547-59 (2004).

9. DuBois, G. & Stephenson, R.A. Sulfonylamine-mediated sulfamation of amines. A mild, high yield synthesis of sulfamic acid salts. *J. Org. Chem.* **45**, 5371-5373 (1980).

10. Kaiser, E.T. & Zaborsky, O.R. Hydrolysis of esters of sulfur-containing acids in oxygen-18 enriched media. *J. Am. Chem. Soc.* **90**, 4626-4628 (1968).

11. Leheste, J.R. *et al*. Megalin knockout mice as an animal model of low molecular weight proteinuria. *Am. J. Pathol.* **155**, 1361-70 (1999).

12. Mori, K.*et al*. Endocytic delivery of lipocalin-siderophore-iron complex rescues the kidney from ischemia-reperfusion injury. *J. Clin. Invest.* **115**, 610-621 (2005).